Original Article

# Improvement of idiopathic pulmonary fibrosis through a combination of *Astragalus* radix and *Angelica sinensis* radix via mammalian target of rapamycin signaling pathway-induced autophagy in rat

**Chao Sun[1#], Huaman Liu[2#], Baihong Chi[3], Jia Han[2], Yasuhiko Koga[4], Kamyar Afshar[5], Xue Liu[2]**

[1]Department of Disease Prevention, The Second Affiliated Hospital of Shandong University of Traditional Chinese Medicine, Jinan, China; [2]Department of Pulmonary and Critical Care Medicine, Affiliated Hospital of Shandong University of Traditional Chinese Medicine, Jinan, China; [3]Department of Pulmonary and Critical Medicine, People's Hospital Rizhao, Rizhao, China; [4]Department of Allergy and Respiratory Medicine, Gunma University Graduate School of Medicine, Gunma, Japan; [5]Division of Pulmonary, Critical Care, and Sleep Medicine, University of California San Diego, La Jolla, CA, USA

*Contributions:* (I) Conception and design: C Sun, X Liu; (II) Administrative support: H Liu; (III) Provision of study materials or patients: J Han; (IV) Collection and assembly of data: All authors; (V) Data analysis and interpretation: All authors; (VI) Manuscript writing: All authors; (VII) Final approval of manuscript: All authors.

[#]These authors contributed equally to this work as co-first authors.

*Correspondence to:* Xue Liu, MD. Department of Pulmonary and Critical Care Medicine, Affiliated Hospital of Shandong University of Traditional Chinese Medicine, No. 42 Wenhua West Road, Lixia District, Jinan 250011, China. Email: liuxue00819855@126.com.

**Background:** There is a major need for effective, well-tolerated treatments for idiopathic pulmonary fibrosis (IPF) in clinic. *Astragalus* radix (AR; Huangqi) and *Angelica sinensis* radix (AS; Danggui) have been frequently used in the treatment of IPF. This study aimed to reveal the pharmacological effects and the mechanisms of the action of an AR-AS combination in treating IPF.

**Methods:** Sprague-Dawley rats were randomly divided into six groups (n=5): control, bleomycin (BLM) model, AR, AS, AR + AS, and prednisone (PDN) groups. A transforming growth factor-β1 (TGF-β1)-induced MRC-5 cell model were also used. Pulmonary fibrosis, inflammation, oxidative stress, and autophagy were evaluated by performing hematoxylin and eosin (H&E) staining, Masson staining, immunohistochemical staining, quantitative real-time polymerase chain reaction (qRT-PCR), Western blotting, enzyme-linked immunosorbent assay (ELISA), immunofluorescence, and hydroxyproline assay following the treatment of AR, AS, and the AR-AS herb pair.

**Results:** Rats administered the AR-AS herb pair had lower α-smooth muscle actin (α-SMA), collagen I, fibronectin, and vimentin levels in lung tissues, and lower inflammatory cytokine levels in rat serum. In addition, the AR-AS herb pair induced mammalian target of rapamycin (mTOR)-mediated autophagy and reduced oxidative stress in BLM-induced rats. The effects of the AR and AS combination were confirmed in MRC-5 cells treated with TGF-β1. Specifically, the combination of AR and AS attenuated MRC-5 cell fibrosis, inflammation, and oxidative stress while inducing autophagy.

**Conclusions:** The combination of AR and AS protects against IPF by inducing autophagy via inhibiting the mTOR signaling pathway. The synergistic action of AR and AS is superior to that of either AR or AS alone.

**Keywords:** *Astragalus* radix (AR); *Angelica sinensis* radix (AS); autophagy; pulmonary fibrosis

Submitted Jan 05, 2024. Accepted for publication Feb 18, 2024. Published online Feb 27, 2024.
doi: 10.21037/jtd-24-28
**View this article at:** https://dx.doi.org/10.21037/jtd-24-28

## Introduction

Idiopathic pulmonary fibrosis (IPF) is a fatal interstitial lung disease characterized by progressive dyspnea and cough, increased oxygen requirements, and restrictive physiology in spirometry (1). IPF is more common in older male adults who are either current or former smokers with a poor prognosis (2). Although the antiproliferative drugs, pirfenidone and nintedanib, can slow progression of lung function and lessen exacerbation events, the therapeutic effect is limited (3). These medications have several adverse drug events that limit tolerability. The costs may also be prohibitive. Thus far, lung transplantation is the only curative measure. A significant number of patients, however, are ineligible for lung transplant due to age, active malignancy, and other co-morbid conditions. Unfortunately, even those who do receive lung transplantation, have a lower survival time compared to those who receive lung transplantation for other types of underlying lung diseases (4,5). Hence, there is an urgent need to investigate new therapeutic approaches. Traditional Chinese medicine has been reviewed as a potentially viable therapeutic option for IPF (6,7). Autophagy is a cell self-renewal process that is fundamental for intracellular degradation and essential for maintaining cell homeostasis (8). Pulmonary diseases, such as IPF, pulmonary hypertension, and cystic fibrosis, are associated with autophagy (9). Overactivation of mammalian target of rapamycin (mTOR) leads to the dysregulation of autophagy in IPF (10). The suppression of autophagy measured by the induced phosphorylation of mTOR and the reduced expression of light chain 3 (LC3) II have been observed in cell lines from patients with lung transplant for IPF (11).

*Astragalus* radix (AR; Huangqi) and *Angelica sinensis* radix (AS; Danggui) are traditional Chinese medicinal herbs, famous for tonifying qi and replenishing blood, respectively (12,13). The combination of AR and AS is commonly used to treat multiple human diseases (14). The combination of AR and AS ameliorates the interferon-γ (IFN-γ)-induced immune destruction of hematopoiesis in bone marrow cells (15). The composition of AR, AS, and *Caulis lonicerae* regulates inflammation of collagen-induced arthritis (16). The AR-AS herb pair has been widely used in clinical practice for patients with IPF (6). Clinical studies on the treatment of IPF used herbal medicine included RA and AS as the main components and have obtained good curative effect (6,17). A previous study has shown that AR weakens renal fibrosis through regulating the transforming growth factor-β1 (TGF-β1)-SMAD signaling pathway in mice and HK2 cells (18). AS and *Hedysarum* radix attenuates myocardial fibrosis induced by radiation (19). However, the mechanism of AR and AS in ameliorating IPF has not been clearly established.

In this study, we investigated whether the AR-AS herb pair protects IPF rats from lung inflammation and fibrosis and whether it can regulate intracellular collagen deposition by inducing autophagy. We present this article in accordance with the ARRIVE reporting checklist (available at https://jtd.amegroups.com/article/view/10.21037/jtd-24-28/rc).

### Highlight box

**Key findings**

- The combination of *Astragalus* radix (AR) and *Angelica sinensis* radix (AS) inhibits pulmonary fibrosis via inducing autophagy.

**What is known and what is new?**

- AR and AS are traditional Chinese medicinal herbs, and have been frequently used in the treatment of idiopathic pulmonary fibrosis (IPF).
- Our study revealed that the combination of AR and AS attenuates pulmonary fibrosis and inflammation. The combination of AR and AS reduces oxidative stress and induces mammalian target of rapamycin-mediated autophagy in the lung during fibrosis.

**What is the implication, and what should change now?**

- These findings provided us a pharmacodynamics comparison result between AR, AS, and the AR-AS herb pair. One of the mechanisms of the combination of AR and AS in treating IPF was revealed. We need to embark on a more in-depth pharmacological study of AR and AS to determine the complex compound ingredients.

## Methods

### *Preparation of freeze-dried AR and AS water extract*

AR and AS were purchased from Shanghai Yuanye Biotechnology Co., Ltd. (Shanghai, China) and identified by a pharmacist of the Affiliated Hospital of Shandong University of Traditional Chinese Medicine. The herbs were crushed to a coarse powder. AR powder (300 g) and AS powder (60 g) were mixed evenly, 50% ethanol was added to the powder, and three types of reflux extraction were conducted: (I) extraction in a 10× volume of 50% ethanol for 2 h; (II) extraction in an 8× volume of 50% ethanol for 1 h; and (III) extraction in a 6× volume of 50% ethanol for 1 h. The extracts were combined and concentrated to a relative density of 1.05 to 1.15 and spray-dried to form a

powder. Treatment with 5 mg of prednisone (PDN) acetate tablets (Zhejiang Xianju Pharmaceutical Co., Ltd., Taizhou, China) was used as the positive control. PDN was dissolved in saline to make a suspension of 4.2 g/L, which was stored in a refrigerator at 4 ℃ for later use.

### *BLM-induced IPF rat model*

Animal experiments were performed under a project license (No. 2021-069) granted by the Animal Ethics Committee of the Affiliated Hospital of Shandong University of Traditional Chinese Medicine, in compliance with the guidelines for the care and use of animals of Shandong University of Traditional Chinese Medicine. A protocol was prepared before the study without registration. Male Sprague-Dawley rats (weight 180±20 g) were purchased from Jinan Pengyue Laboratory Animal Breeding Co., Ltd. (Jinan, China). Rats were randomly divided into six groups (n=5). The model of pulmonary fibrosis was established via intratracheal instillation of bleomycin (BLM; Shanghai Yuanye Biotechnology Co., Ltd.). The rats were injected intraperitoneally with 1.5% pentobarbital sodium (30 mg/kg) and then fixed on the 35° inclined plate after anesthesia. The skin was routinely sterilized with 75% medical alcohol. The skin was cut 2–3 cm from the middle line of the neck, and the muscle was bluntly separated to expose the trachea. A 4-gauge needle was inserted into the trachea from the space of centripetal tracheal cartilage, and 0.3 mL of BLM (5 mg/kg) was infused into the trachea through a micropump at a rate of 2 mL/h. Following this, the plate was quickly rotated upright and for 3 min to ensure the BLM was evenly distributed in the lungs. After suturing of the muscle and skin, disinfection was again applied, and penicillin sodium was injected intraperitoneally to prevent infection. In the control group, only normal saline was injected into the trachea, with the other steps being the same as those of modeling.

### *Animal grouping and administration*

The rats were randomly divided into control group, model group (BLM), qi-invigorating (AR) group, blood-activation (AS) group, qi-invigorating and blood-activation (AR + AS) group, and PDN group. Except for the control group, the groups were pulmonary fibrosis models. From the second day after BLM injection, the control group and the model group were gavaged with saline (10 mL/kg) once a day. The PDN group was given PDN suspension (4.2 mg/kg) by gavage. The AR group, the AS group, and the AR + AS group were given 1.35, 1.35, and 2.7 g/kg/d concentrated powder, respectively. The rats were gavaged for 28 days. Subsequently, the lungs were isolated. The upper and middle lobes of the lungs were fixed in 4% paraformaldehyde and embedded in paraffin for pathological and immunohistochemical detection. The lower lobes of the lungs were frozen at −80 ℃ for Western blotting.

### *Hematoxylin and eosin (H&E) staining and Masson staining*

The embedded lungs were sliced into 5-μm sections and stained with a H&E kit (Servicebio, Wuhan, China) or Masson staining kit (Servicebio, Wuhan,) according to the instructions of the kit. Images were obtained under a NIKON Ni-U microscope. (20).

### *Immunohistochemistry*

α-smooth muscle actin (α-SMA; 1:500, #19245, CST, Danvers, MA, USA) and collagen I (1:500, #72026, CST) were added to the sections. The sections were stained with streptavidin-peroxidase horseradish peroxidase (HRP) and hematoxylin and detected under a microscope.

### *Reactive oxygen species (ROS) production*

Frozen lung tissues were cut into sections. MRC-5 cells were seeded into 12-well plates overnight. The sections and cells were treated with 5 μM of the ROS probe dichlorodihydrofluorescein diacetate (DCFH-DA; S0033S, Beyotime, Shanghai, China) for 30 min at 37 ℃ in the dark. The sections and cells were detected under a fluorescence microscope.

### *Hydroxyproline assay*

After hydrolysis of right lung tissues in the 2 mL of extraction solution, the pH of samples adjusts to 6.5 to 8.0 using 10 mol/L NaOH. The level of hydroxyproline was measured with a hydroxyproline assay kit (#BC0250, Solarbio, Beijing, China) at 560 nm.

### *MRC-5 cell culture and treatment*

The MRC-5 cells were purchased from Wuhan Procell Life Technology Co., Ltd. (Wuhan, China) and cultured

**Table 1** The primer sequences used for qRT-PCR

| Primer (human) | Sequence (5'→3') |
|---|---|
| ACTA2 | |
| Forward primer | CTGAAGAGCATCCCACCCTG |
| Reverse primer | TCCAGCACGATGCCAGTTG |
| COL1A1 | |
| Forward primer | CTCGTGGAAATGATGGTGCT |
| Reverse primer | ACCAGGTTCACCGCTGTTAC |
| FN1 | |
| Forward primer | CCGCCGAATGTAGGACAAGA |
| Reverse primer | GACAGAGTTGCCCACGGTAA |
| VIM | |
| Forward primer | CTCCCTGAACCTGAGGGAAAC |
| Reverse primer | TTGCGCTCCTGAAAAACTGC |
| TNF-α | |
| Forward primer | CCCATGTTGTAGCAAACCCT |
| Reverse primer | CTGGAAGACCCCTCCCAGAT |
| IL-1β | |
| Forward primer | CCAAACCTCTTCGAGGCACA |
| Reverse primer | GCTGCTTCAGACACTTGAGC |
| IL-6 | |
| Forward primer | CCGGGAACGAAAGAGAAGCTC |
| Reverse primer | ACCGAAGGCGCTTGTGGAG |
| LC3 | |
| Forward primer | GAGTTACCTCCCGCAGCC |
| Reverse primer | GCTCGATGATCACCGGGATTT |
| GAPDH | |
| Forward primer | AATGGGCAGCCGTTAGGAAA |
| Reverse primer | GCCCAATACGACCAAATCAGAG |

qRT-PCR, quantitative real-time polymerase chain reaction; ACTA2, actin alpha 2, smooth muscle; COL1A1, collagen type I alpha 1 chain; FN1, fibronectin 1; VIM, vimentin; LC3, light chain 3; TNF-α, tumor necrosis factor-α; IL, interleukin; LC3, light chain 3; GAPDH, glyceraldehyde-3-phosphate dehydrogenase.

in minimum essential medium (MEM) containing 10% fetal bovine serum and 1% penicillin and streptomycin at 37 ℃. The cells were divided into five groups: a control group, TGF-β1 group, qi-invigorating (AR) group, blood-activation (AS) group, and qi-invigorating and blood-activation (AR + AS) group. MRC-5 cells at $5\times10^4$ cells/well were pretreated with 100 μg/mL AR, AS, or AR + AS for 1 h, and then TGF-β1 (5 ng/mL) was added to each well for 24 h. MRC-5 cells were treated with 3-methyladenine (3-MA; 1 mM; MedChemExpress, Monmouth Junction, NJ, USA) for 1 h prior to TGF-β1 treatment.

### *Enzyme-linked immunosorbent assay (ELISA)*

According to the ELISA kit's instructions, the levels of tumor necrosis factor-α (TNF-α), interleukin (IL)-1β, IL-6, and TGF-β1 in rat serum (TNF-α: E-EL-R2856, Elabscience, Wuhan, China; IL-1β: E-EL-R0012, Elabscience; IL-6: #P6276, Beyotime; TGF-β1: #PT878, Beyotime) were determined at 450 nm in a microplate reader.

### *Immunofluorescence*

MRC-5 cells were grown on the glass-bottom slides in six-well plates, fixed in 4% paraformaldehyde, and permeated with 0.2% Triton X-100. Cells were incubated with antibody against LC3 (1:200, #12741, CST) at 4 ℃ overnight and incubated with Alexa Fluor® 488 Conjugate secondary antibody for another 1.5 h at room temperature. The cells were stained with 4',6-diamidino-2-phenylindole (DAPI; #D8200, Solarbio) and observed under a fluorescence microscope.

### *Assessment of superoxide dismutase (SOD), malondialdehyde (MDA), and glutathione (GSH)*

A SOD assay kit (#BC0175, Solarbio), MDA assay kit (#BC0025, Solarbio), and GSH assay kit (#BC1175, Solarbio) were used to determine the relative levels of SOD, MDA, and GSH, respectively.

### *Quantitative real-time polymerase chain reaction (qRT-PCR)*

Total RNA of MRC-5 cells was extracted using RNA isolater (#R401-01, Vazyme, Nanjing, China). RNA was reverse-transcribed into complement DNA (cDNA), and qRT-PCR was perfomed using a HiScript II One Step qRT-PCR SYBR Green Kit (#Q221-01, Vazyme). The primer sequences are listed in *Table 1*. Expression was normalized using the using $2^{-\Delta\Delta Ct}$ method.

### *Western blotting*

Proteins were extracted from lung tissues and MRC-5 cells using RIPA buffer (Beyotime). The concentrations were determined with BCA Protein Assay Kit (Beyotime). Proteins were separated using sodium dodecyl sulfate-polyacrylamide gel electrophoresis (SDS-PAGE) and transferred onto polyvinylidene fluoride (PVDF) membranes. Thereafter, membrane blocking was completed with 5% skim milk for 1 h and incubated with α-SMA (#19245, CST), collagen I (#91144, CST), fibronectin (ab268020, Abcam), vimentin (#5741, CST), phospho-mTOR (p-mTOR; #2971, CST), mTOR (ab32028, Abcam, Cambridge, UK), LC3 (#12741, CST), TNF-α (ab307164, Abcam), IL-1β (ab315084, Abcam), IL-6 (ab9324, Abcam), and glyceraldehyde-3-phosphate dehydrogenase (GAPDH) (60004-1-Ig, Proteintech, Rosemont, IL, USA) at 4 ℃ overnight. After washing, the sample was incubated with HRP-conjugated immunoglobin G (IgG) antibody (#7074, CST) at room temperature for 1.5 h. The blots were detected using and enhanced chemiluminescence (ECL) system (#E411-04/05, Vazyme).

### *Statistical analysis*

Data are presented as the mean ± standard deviation (SD) of three independent experiments. GraphPad Prism 8.0 (GraphPad Software, Inc., San Diego, CA, USA) was used for statistical analysis. The differences between groups were evaluated using analysis of variance, followed by the Tukey test. $P<0.05$ was considered statistically significant.

## Results

### *The combination of AR and AS attenuated IPF in BLM-induced rats*

To explore the role of AR and AS in inflammation and fibrosis, we treated rats with BLM (*Figure 1A*). As indicated by HE staining, we observed alveolar collapse, fibroblast proliferation, and collagen deposition in the fibrotic area in the lung of BLM-induced rats. The degree of alveolitis and pulmonary fibrosis in the AR or AS groups was significantly decreased, and the AR + AS group exhibited less pulmonary injury compared with the BLM, AR, and AS groups (*Figure 1B,1C*). Similarly, the Masson staining showed collagen deposition in the lung of BLM-induced rats. The rats treated with the combination of AR and AS showed a reduction of pulmonary fibrosis comparable to those treated with PDN and a more reduction of pulmonary fibrosis compared to the rats subjected to AR treatment or AS treatment alone (*Figure 1D,1E*). Notably, the AR-AS combination attenuated BLM-induced aggregation of hydroxyproline in rats (*Figure 1F*). AR-AS combination therapy significantly attenuated pulmonary fibrosis in BLM-induced rats.

### *The combination of AR and AS attenuated pulmonary fibrosis and inflammation in rats*

Immunohistochemical analysis (*Figure 2A-2D*) showed that the BLM-induced increases in α-SMA and collagen I in lung sections were attenuated by AR, AS, and the AR-AS herb pair. The AR-AS herb pair had a more significant inhibitory effect on α-SMA and collagen I protein expression, and the inhibitory effect was similar to that of PDN. Consistent with the immunohistochemical results, the expression of α-SMA, collagen I, fibronectin, and vimentin was decreased in the lung tissues of the AR-AS herb pair-treated rats (*Figure 2E,2F*). Furthermore, the AR-AS herb pair exerted a greater reduction of TGF-β1, TNF-α, IL-1β, and IL-6 levels compared with AR or AS, and the inhibitory effect was similar to that of PDN (*Figure 2G*). This result demonstrates that the AR-AS herb pair could suppress pulmonary fibrosis and inflammation in BLM-induced rats.

### *The combination of AR and AS reduced oxidative stress and induced mTOR-mediated autophagy in rats*

Western blot results showed that AR or AS led to notable attenuation in mTOR activation and promotion in the transition of LC3I to LC3II. The AR-AS herb pair and PDN treatment significantly reduced the phosphorylation of mTOR and induced LC3I to LC3II transition as compared to AR or AS treatment alone (*Figure 3A*). The AR-AS herb pair also decreased the MDA level and enhanced SOD and GSH levels in the BLM-induced rats (*Figure 3B*). These findings demonstrate that the AR-AS herb pair inhibits oxidative stress and activates autophagy in fibrotic lungs.

### *The combination of AR and AS inhibited MRC-5 cell fibrosis and inflammation induced by TGF-β1*

To more finely characterize the efficacy of the AR-AS herb pair on fibrosis and inflammation, we treated MRC-5 cells

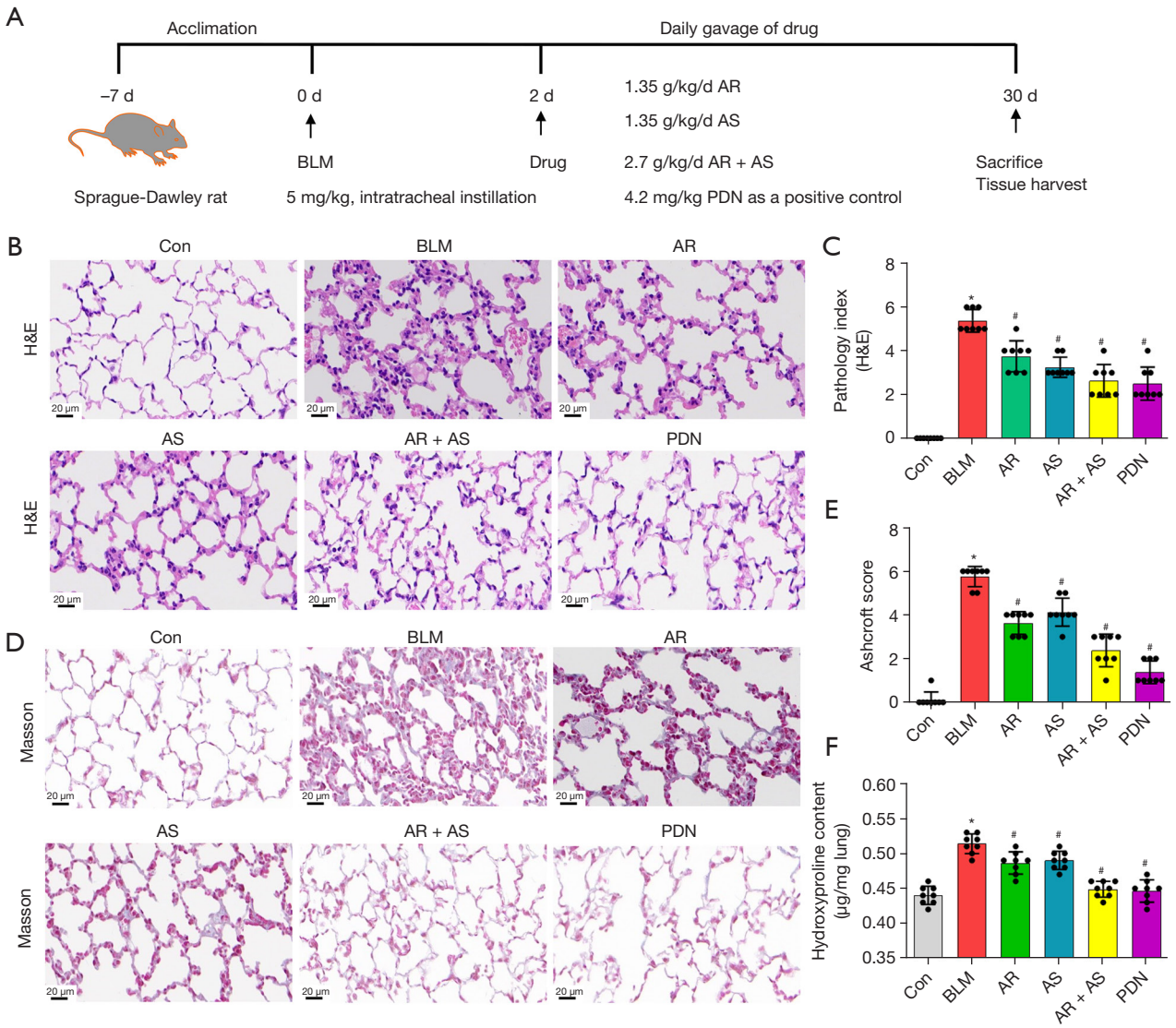


**Figure 1** The combination of AR and AS attenuated IPF in BLM-induced rats. (A) A flowchart describes the research procedures of this study. Lung sections were stained with H&E (B) or Masson trichrome (D) to assess collagen accumulation, and the pathology index (C) and Ashcroft score (E) were quantified. (F) The level of hydroxyproline was measured in lung tissue. *, P<0.05 versus the control group; #, P<0.05 versus the BLM group. BLM, bleomycin; AR, *Astragalus* radix; AS, *Angelica sinensis* radix; PDN, prednisone; Con, control; H&E, hematoxylin and eosin; IPF, idiopathic pulmonary fibrosis.

with TGF-β1. The results in *Figure 4A,4B* demonstrated that the messenger RNA (mRNA) and protein levels of α-SMA, collagen I, fibronectin, and vimentin were remarkably increased in the TGF-β1-induced MRC-5 cells, and these increases were inhibited by AR, AS, and the AR-AS herb pair treatment. Furthermore, the mRNA and protein levels of TNF-α, IL-1β, and IL-6 were markedly upregulated in TGF-β1-treated MRC-5 cells, and their upregulation was inhibited by AR, AS, and AR-AS herb pair treatment (*Figure 4C,4D*), with the effect of the AR-AS herb pair being the most prominent.

### *The combination of AR and AS induced mTOR-mediated autophagy in TGF-β1-treated MRC-5 cells*

The mRNA level of *LC3* was decreased in TGF-β1-treated MRC-5 cells and markedly increased in cells treated with AR, AS, or the AR-AS herb pair (*Figure 5A*). AR, AS, and

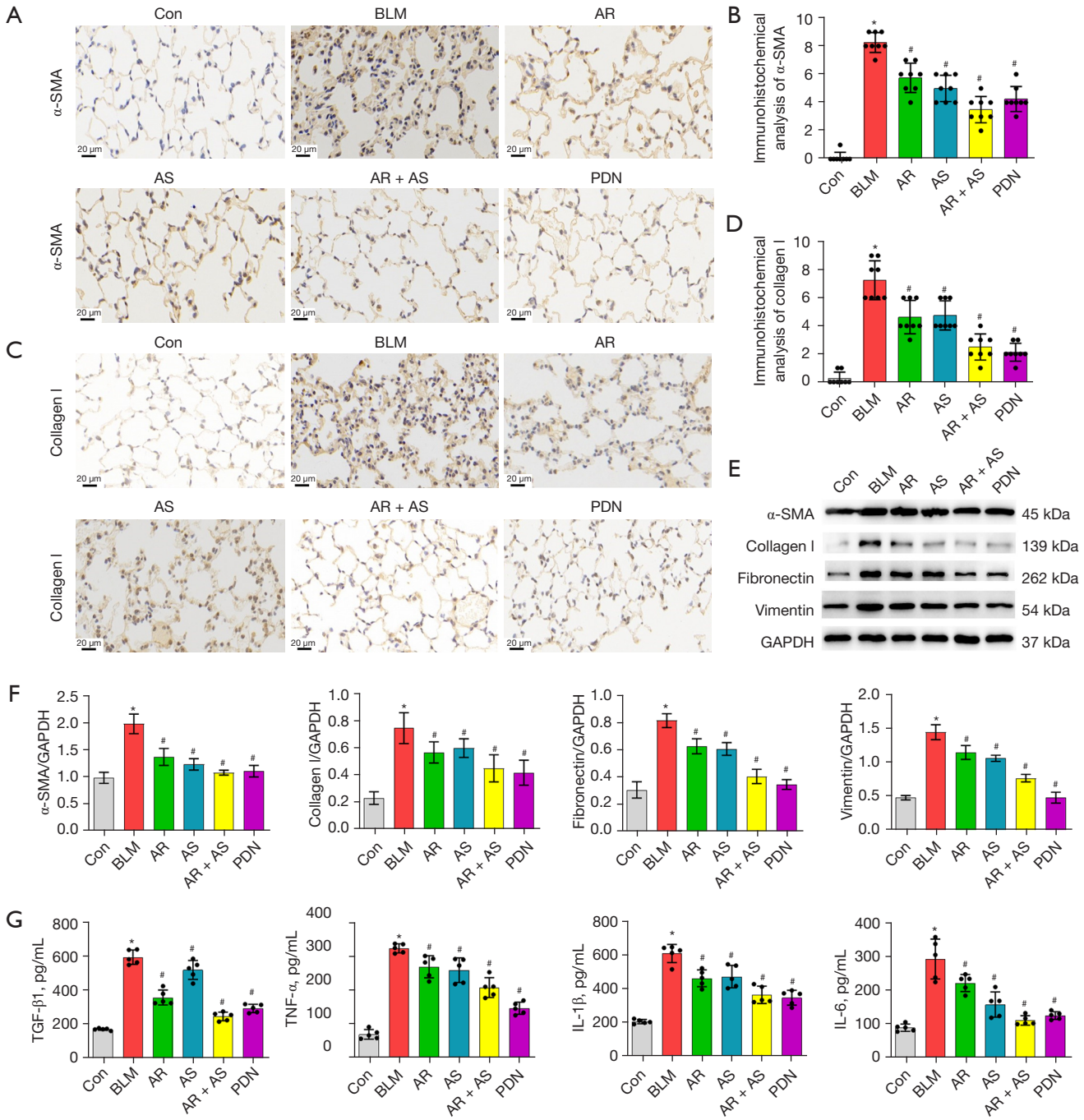


**Figure 2** The combination of AR and AS attenuated pulmonary fibrosis and inflammation in rats. (A-D) The protein levels of α-SMA and collagen were evaluated via immunohistochemistry. (E,F) The protein levels of α-SMA, collagen I, fibronectin, and vimentin were detected via Western blotting. (G) TGF-β1, TNF-α, IL-1β, and IL-6 levels were detected via ELISA. *, P<0.05 versus the control group; #, P<0.05 versus the BLM group. Con, control; BLM, bleomycin; AR, *Astragalus* radix; α-SMA, α-smooth muscle actin; AS, *Angelica sinensis* radix; PDN, prednisone; GAPDH, glyceraldehyde-3-phosphate dehydrogenase; TGF-β1, transforming growth factor-β1; TNF-α, tumor necrosis factor-α; IL, interleukin; ELISA, enzyme-linked immunosorbent assay.

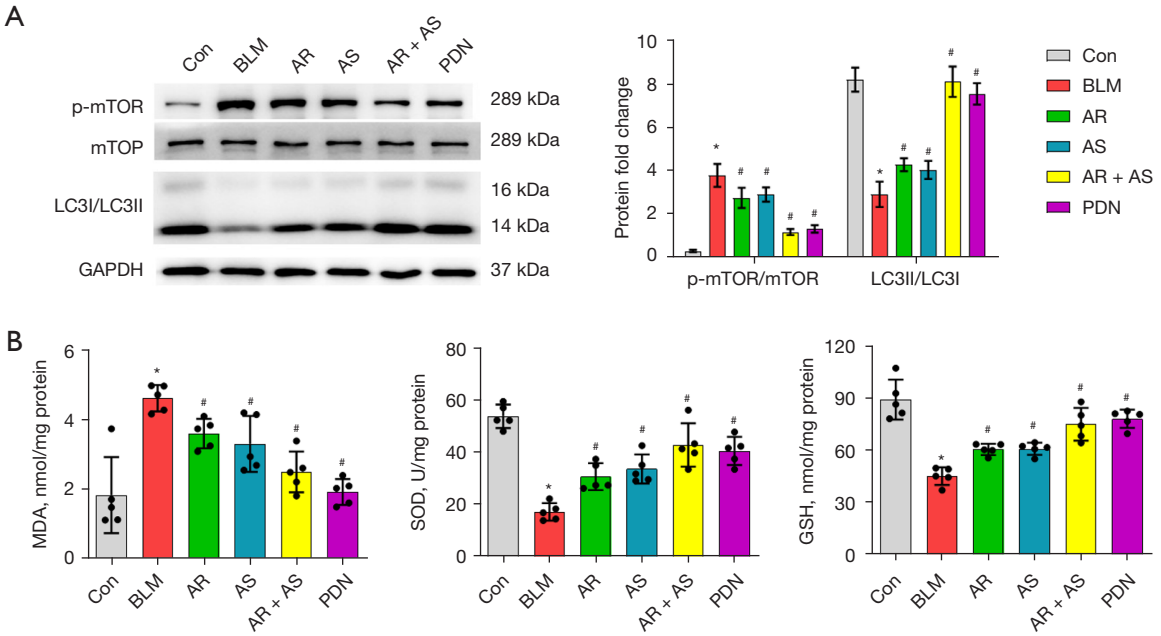


**Figure 3** The combination of AR and AS reduced the oxidative stress and induced mTOR-mediated autophagy in rats. (A) The protein levels of p-mTOR, mTOR, and LC3 were measured with Western blotting. (B) MDA, SOD, and GSH levels in lung tissue were detected. *, P<0.05 versus the control group; #, P<0.05 versus the BLM group. Con, control; BLM, bleomycin; AR, *Astragalus* radix; AS, *Angelica sinensis* radix; PDN, prednisone; p-mTOR, phospho-mTOR; mTOR, mammalian target of rapamycin; LC3, light chain 3; GAPDH, glyceraldehyde-3-phosphate dehydrogenase; MDA, malondialdehyde; SOD, superoxide dismutase; GSH, glutathione.

AR-AS herb pair treatment suppressed the phosphorylation of mTOR and promoted the ratio of LC3II to LC3I in cells treated with TGF-β1 (*Figure 5B*). AR, AS, and the AR-AS herb pair enhanced LC3 expressing as indicated by immunofluorescence (*Figure 5C*). As presented in *Figure 5D*, TGF-β1 exposure increased the accumulation of ROS in MRC-5 cells, and AR, AS, and AR-AS herb pair treatment decreased the accumulation of ROS in MRC-5 cells. Similarly, AR, AS, and the AR-AS herb pair treatment also suppressed the MDA level and promoted SOD and GSH levels in the TGF-β1-induced MRC-5 cells (*Figure 5E*). The effect of the AR-AS herb pair was the most obvious among these treatment groups.

### *The combination of AR and AS inhibited MRC-5 cell fibrosis via inducing autophagy*

To further examine the protective effects of the AR-AS herb pair in lung fibrosis, we treated MRC-5 cells with 3-MA. The mRNA and protein levels of α-SMA, collagen I, fibronectin, and vimentin were inhibited by AR, AS, and the AR-AS herb pair treatment in TGF-β1-treated cells, which was blocked by 3-MA (*Figure 6A,6B*). AR, AS, and the AR-AS herb pair reduced TGF-β1-stimulated inflammatory factor expression, including TNF-α, IL-1β, and IL-6, which was reversed by 3-MA (*Figure 6C,6D*).

## Discussion

IPF is a progressive and lethal interstitial lung disease characterized by a worsening condition of the fibrotic lung changes on chest images, restrictive spirometric changes, increased dyspnea, and worsened functional status leading to respiratory failure and death (21,22). There are few therapeutic options for IPF, and consequently, herbs from traditional Chinese medicine have considerable potential for IPF treatment. The AR-AS herb pair has been used in clinic for IPF and found to be effective for the protection of lung function (6). It is vital to systematically investigate the mechanism of antifibrosis action of the AR-AS herb pair as potential options for patients with IPF. In this study, we found that the AR-AS herb pair could alleviate pulmonary fibrosis by inhibiting collagen deposition, inflammatory activation, and oxidative stress and by inducing mTOR-

 

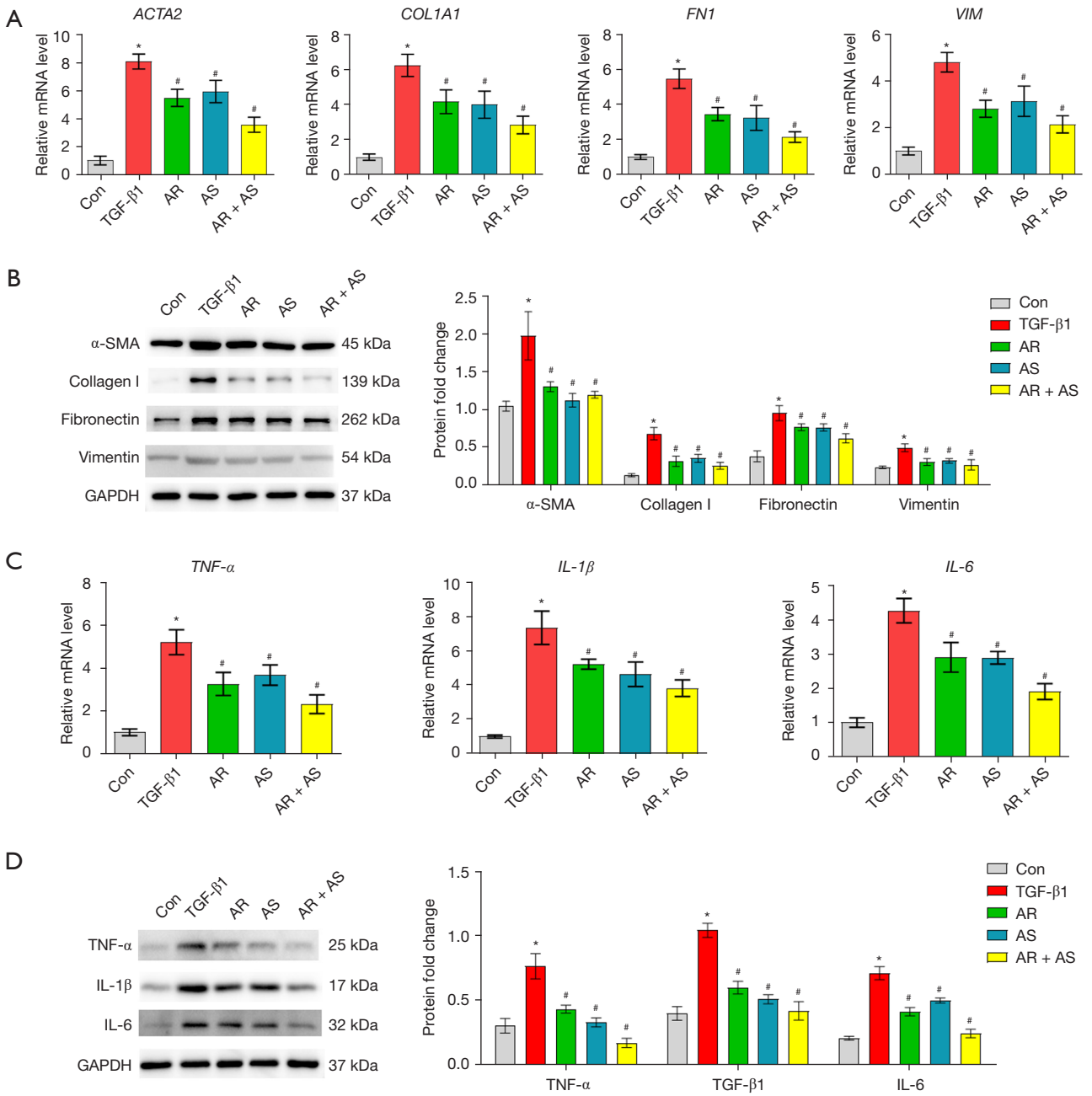


**Figure 4** The combination of AR and AS inhibited MRC-5 cell fibrosis and inflammation induced by TGF-β1. (A,B) The mRNA and protein levels of α-SMA, collagen I, fibronectin, and vimentin were measured via qRT-PCR and Western blotting. (C,D) TNF-α, IL-1β, and IL-6 levels of mRNA and protein were detected with qRT-PCR and Western blotting. *, P<0.05 versus the control group; #, P<0.05 versus the TGF-β1 group. Con, control; TGF-β1, transforming growth factor-β1; AR, *Astragalus* radix; AS, *Angelica sinensis* radix; mRNA, messenger RNA; ACTA2, actin alpha 2, smooth muscle; COL1A1, collagen type I alpha 1 chain; FN1, fibronectin 1; VIM, vimentin; α-SMA, α-smooth muscle actin; GAPDH, glyceraldehyde-3-phosphate dehydrogenase; TNF-α, tumor necrosis factor-α; IL, interleukin; qRT-PCR, quantitative real-time polymerase chain reaction.

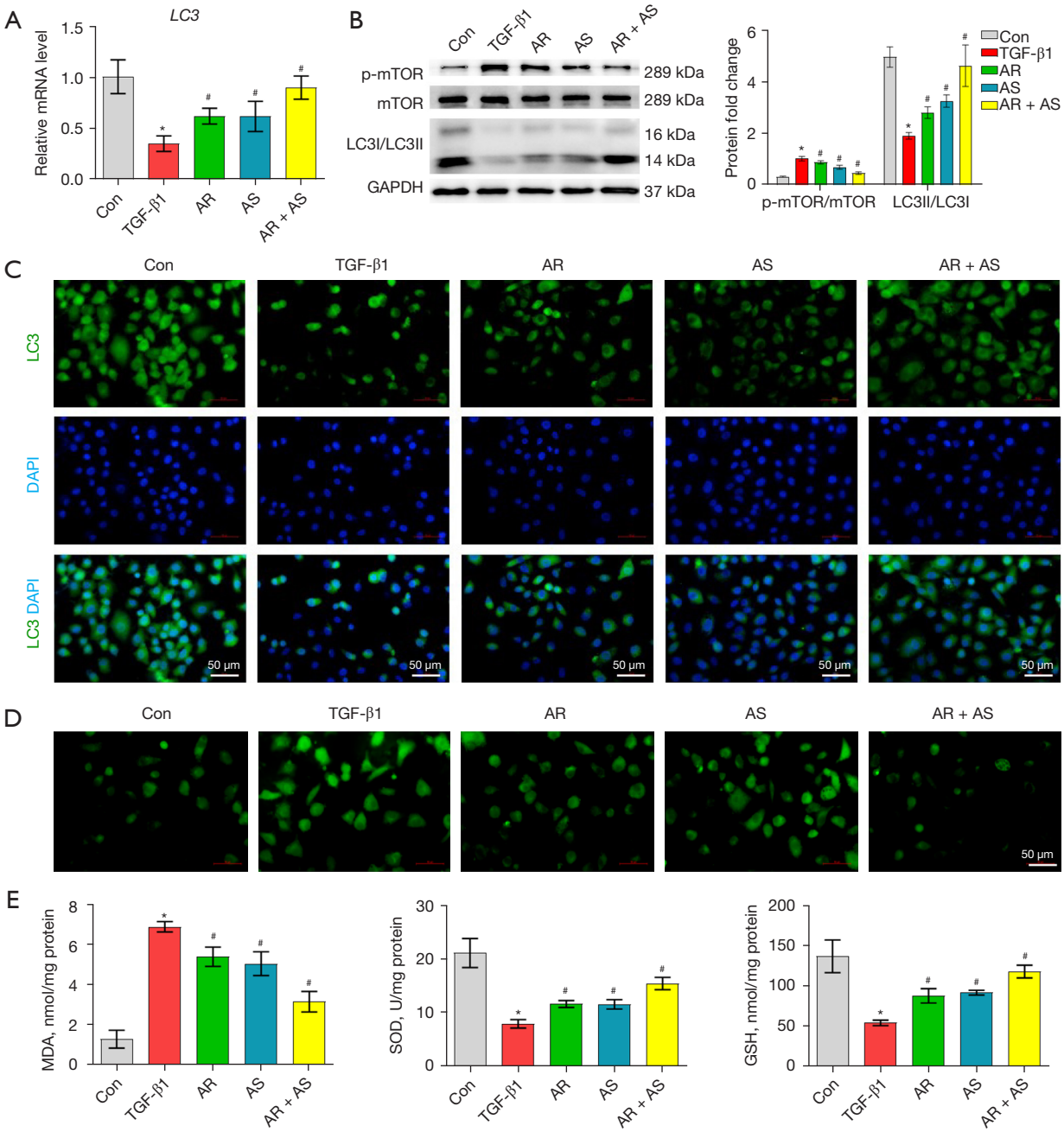


**Figure 5** The combination of AR and AS induced mTOR-mediated autophagy in TGF-β1-treated MRC-5 cells. (A) LC3 mRNA was detected with qRT-PCR. (B) The protein levels of p-mTOR, mTOR, and LC3 were measured with Western blotting. (C) LC3 expression was measured by immunofluorescent staining. (D) ROS detected with DCFH-DA staining. (E) MDA, SOD, and GSH levels measured by ELISA. *, P<0.05 versus the control group; #, P<0.05 versus the TGF-β1 group. Con, control; TGF-β1, transforming growth factor-β1; AR, *Astragalus* radix; AS, *Angelica sinensis* radix; mRNA, messenger RNA; LC3, light chain 3; p-mTOR, phospho-mTOR; mTOR, mammalian target of rapamycin; GAPDH, glyceraldehyde-3-phosphate dehydrogenase; DAPI, 4',6-diamidino-2-phenylindole; MDA, malondialdehyde; SOD, superoxide dismutase; GSH, glutathione; qRT-PCR, quantitative real-time polymerase chain reaction; ROS, reactive oxygen species; DCFH-DA, dichlorodihydrofluorescein diacetate; ELISA, enzyme-linked immunosorbent assay.

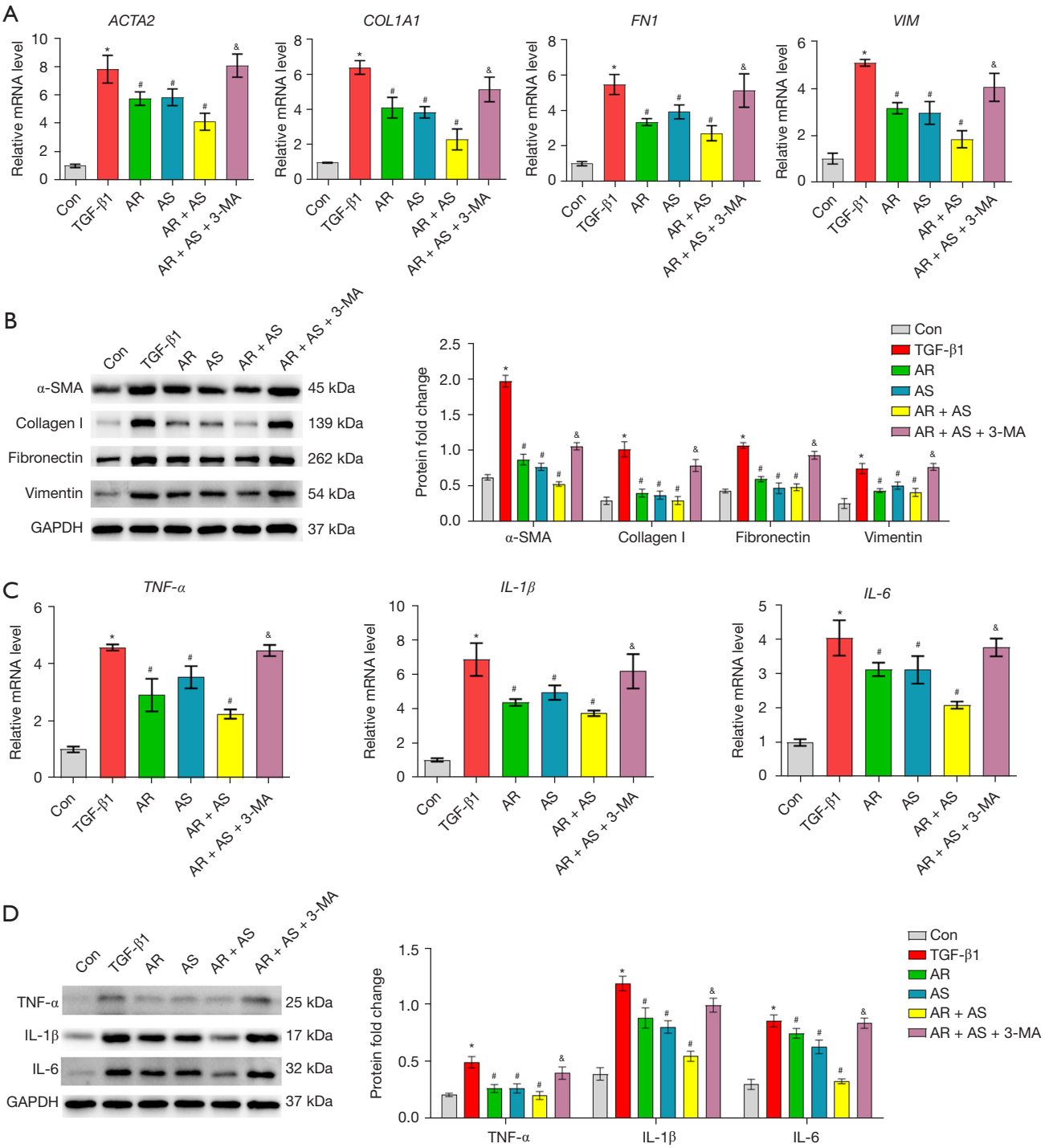


**Figure 6** The combination of AR and AS inhibited MRC-5 cell fibrosis via inducing autophagy. (A,B) The mRNA and protein levels of α-SMA, collagen I, fibronectin, and vimentin were measured with qRT-PCR and Western blotting. (C,D) TNF-α, IL-1β, and IL-6 levels of mRNA and protein were detected with qRT-PCR and Western blotting. *, P<0.05 versus the control group; #, P<0.05 versus the TGF-β1 group; &, P<0.05 versus the AR + AS group. Con, control; TGF-β1, transforming growth factor-β1; AR, *Astragalus* radix; AS, *Angelica sinensis* radix; 3-MA, 3-methyladenine; mRNA, messenger RNA; α-SMA, α-smooth muscle actin; ACTA2, actin alpha 2, smooth muscle; COL1A1, collagen type I alpha 1 chain; FN1, fibronectin 1; VIM, vimentin; LC3, light chain 3; GAPDH, glyceraldehyde-3-phosphate dehydrogenase; TNF-α, tumor necrosis factor-α; IL, interleukin; qRT-PCR, quantitative real-time polymerase chain reaction.

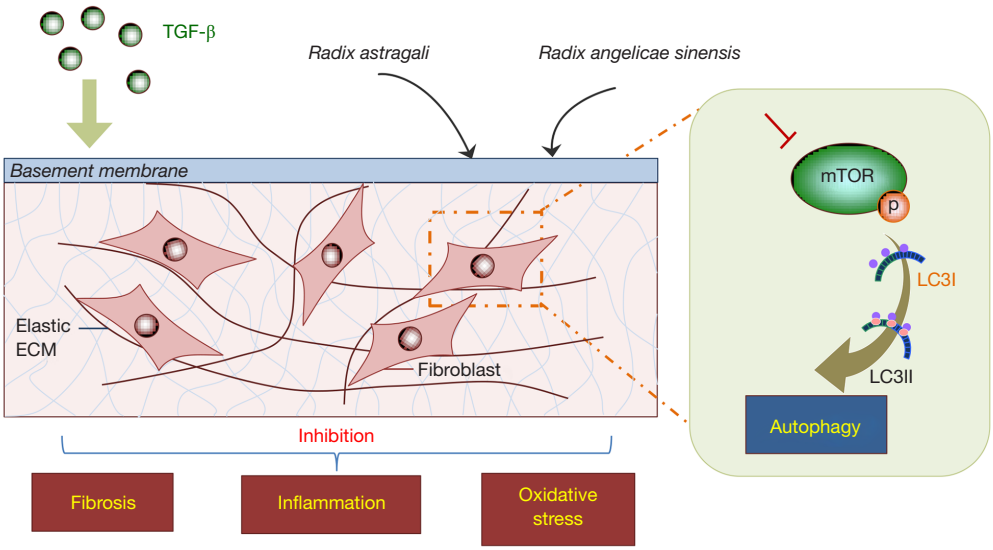


**Figure 7** Mechanisms associated with the effects of the AR-AS herb pair on inhibiting pulmonary fibrosis. TGF-β, transforming growth factor-β; ECM, extracellular matrix; mTOR, mammalian target of rapamycin; LC3, light chain 3; AR, *Astragalus* radix; AS, *Angelica sinensis* radix.

mediated autophagy (*Figure* 7).

Studies have shown that intratracheal injections of BLM in rats and treatment of TGF-β1 in MRC-5 cells can induce collagen deposition and fibrogenic proteins (23,24). The AR-AS herb pair inhibited the expression levels of α-SMA, collagen I, fibronectin, and vimentin, which indicated its strong antifibrotic effects.

Oxidative stress has been shown to play an important role in pulmonary fibrosis progression, and a variety of oxidant and antioxidant processes are altered in the cellular sources participating in IPF (25). ROS contributes prominently to the development of IPF (26). Consequently, several antioxidant therapies have been assayed in animal and cell models (27). One investigation showed that 3-carbamoyl-proxyl nitroxide radicals inhibited the severity of fibrosis in BLM-induced mice (28). Zingerone ameliorates oxidative stress, inflammation, and histopathological damage in BLM-induced pulmonary fibrosis by regulate the expression of TGF-β1 and iNOS (29). The application of the antioxidant effects of AR in injury and disease has been summarized previously (30). AS can exert antioxidant, hematinic, and immunogenic pharmacological activity (31). In this study, the AR-AS herb pair improved BLM-induced IPF by decreasing oxidative stress, with the synergistic action of AR and AS being superior to that of either AR or AS alone.

Inflammation is thought to play a pivotal role in the progression of IPF (32,33). Several herbs have been reported to possess anti-inflammatory properties (34). Wenfei Buqi Tongluo Formula is composed of 13 kinds of Chinese herbs, such as AR and AS, and can suppress inflammation in BLM-induced IPF mice by regulating the Toll-like receptor 4 (TLR4)-myeloid differentiation factor-88 (MyD88)-nuclear factor-κB (NF-κB) pathway (35). Bufei Decoction, which is composed of AR, AS, and other herbs, can alleviate fibrosis by exerting anti-inflammatory activity in IPF mice (36). In this study, the AR-AS herb pair improved the condition of IPF rats in a similar manner. The anti-inflammatory effect of the AR-AS herb pair was the most obvious among the three treatment groups.

Recent research has demonstrated that enhancing autophagy is possible a treatment option for IPF (37-39). One study found that an increase in the ratio of LC3II to LC3I is accompanied by induced autophagy activity and alleviation of lung fibrosis (40), while another found p-mTOR expression to be increased in the IPF fibroblasts of BLM-induced mouse lungs (39). Active ingredients derived from AS and AR have been studied in the treatment of atherosclerosis by inducing autophagy. For instance, the organic acid of *Angelica*, a main active constituent in AS, was demonstrated to increase the expression of LC3II protein in an oxidized low-density lipoprotein model (41). Calycosin, a flavonoid from AR, ameliorates atherosclerosis by inducing

autophagy (42). Consistent with previous studies (43,44), the AR-AS herb pair examined in our study decreased the phosphorylation of mTOR and promoted the radio of LC3II to LC3I in BLM-induced rats and TGF-β1-treated cells. 3-MA, a potent autophagy inhibitor, is widely used for *in vivo* and *in vitro* experimental research (45). In this study, we further verified the antifibrotic effect of the AR-AS herb pair via inducing autophagy by adding 3-MA to the cells.

## Conclusions

The combination of AR and AS can induce autophagy via inhibiting mTOR signaling pathway and alleviating the pulmonary fibrosis, inflammatory reaction, and oxidative stress induced by BLM and TGF-β1. The synergistic action of AR and AS was superior to that of either AR or AS alone and making it a potential therapeutic option for patients with IPF.

## Acknowledgments

*Funding:* This research was funded by the National Natural Science Foundation of China (No. 82004285, to C.S., H.L., J.H., B.C., and X.L.).

## Footnote

*Reporting Checklist:* The authors have completed the ARRIVE reporting checklist. Available at https://jtd.amegroups.com/article/view/10.21037/jtd-24-28/rc

*Data Sharing Statement:* Available at https://jtd.amegroups.com/article/view/10.21037/jtd-24-28/dss

*Peer Review File:* Available at https://jtd.amegroups.com/article/view/10.21037/jtd-24-28/prf

*Conflicts of Interest:* All authors have completed the ICMJE uniform disclosure form (available at https://jtd.amegroups.com/article/view/10.21037/jtd-24-28/coif). Y.K. receives a research grant from the Nippon Boehringer Ingelheim Co., Ltd. C.S., H.L., J.H., B.C., and X.L. report funding support from the National Natural Science Foundation of China (No. 82004285). The other author has no conflicts of interest to declare.

*Ethical Statement:* The authors are accountable for all aspects of the work in ensuring that questions related to the accuracy or integrity of any part of the work are appropriately investigated and resolved. Animal experiments were performed under a project license (No. 2021-069) granted by the Animal Ethics Committee of the Affiliated Hospital of Shandong University of Traditional Chinese Medicine, in compliance with the guidelines for the care and use of animals of Shandong University of Traditional Chinese Medicine.



## References

1. Janowiak P, Szymanowska-Narloch A, Siemińska A. IPF Respiratory Symptoms Management - Current Evidence. Front Med (Lausanne) 2022;9:917973.
2. Kishaba T. Acute Exacerbation of Idiopathic Pulmonary Fibrosis. Medicina (Kaunas) 2019;55:70.
3. Di Martino E, Provenzani A, Vitulo P, et al. Systematic Review and Meta-analysis of Pirfenidone, Nintedanib, and Pamrevlumab for the Treatment of Idiopathic Pulmonary Fibrosis. Ann Pharmacother 2021;55:723-31.
4. Laporta Hernandez R, Aguilar Perez M, Lázaro Carrasco MT, et al. Lung Transplantation in Idiopathic Pulmonary Fibrosis. Med Sci (Basel) 2018;6:68.
5. Stella GM, D'Agnano V, Piloni D, et al. The oncogenic landscape of the idiopathic pulmonary fibrosis: a narrative review. Transl Lung Cancer Res 2022;11:472-96.
6. Zhang Y, Gu L, Xia Q, et al. Radix Astragali and Radix Angelicae Sinensis in the Treatment of Idiopathic Pulmonary Fibrosis: A Systematic Review and Meta-analysis. Front Pharmacol 2020;11:415.
7. Bing P, Zhou W, Tan S. Study on the Mechanism of Astragalus Polysaccharide in Treating Pulmonary Fibrosis Based on "Drug-Target-Pathway" Network. Front Pharmacol 2022;13:865065.
8. Kim KH, Lee MS. Autophagy--a key player in cellular and body metabolism. Nat Rev Endocrinol 2014;10:322-37.
9. Liao SX, Sun PP, Gu YH, et al. Autophagy and pulmonary disease. Ther Adv Respir Dis 2019;13:1753466619890538.

 

10. Lawrence J, Nho R. The Role of the Mammalian Target of Rapamycin (mTOR) in Pulmonary Fibrosis. Int J Mol Sci 2018;19:778.
11. Nho RS, Hergert P. IPF fibroblasts are desensitized to type I collagen matrix-induced cell death by suppressing low autophagy via aberrant Akt/mTOR kinases. PLoS One 2014;9:e94616.
12. Yang F, Qu Q, Zhao C, et al. Paecilomyces cicadae-fermented Radix astragali activates podocyte autophagy by attenuating PI3K/AKT/mTOR pathways to protect against diabetic nephropathy in mice. Biomed Pharmacother 2020;129:110479.
13. Chen XP, Li W, Xiao XF, et al. Phytochemical and pharmacological studies on Radix Angelica sinensis. Chin J Nat Med 2013;11:577-87.
14. Dong TT, Zhao KJ, Gao QT, et al. Chemical and biological assessment of a chinese herbal decoction containing Radix Astragali and Radix Angelicae Sinensis: Determination of drug ratio in having optimized properties. J Agric Food Chem 2006;54:2767-74.
15. Liu J, Wei J, Wang C, et al. The combination of Radix Astragali and Radix Angelicae Sinensis attenuates the IFN-γ-induced immune destruction of hematopoiesis in bone marrow cells. BMC Complement Altern Med 2019;19:356.
16. Feng G, Li D, Liu J, et al. The Herbal Combination of Radix astragali, Radix angelicae sinensis, and Caulis lonicerae Regulates the Functions of Type 2 Innate Lymphocytes and Macrophages Contributing to the Resolution of Collagen-Induced Arthritis. Front Pharmacol 2022;13:964559.
17. Sun ZT, Feng JH, Li XJ, et al. Interference of tonifying qi, activating blood and dispersing accumulation on pulmonary fibrosis and the mechanism research. Journal of Tianjin University of Traditional Chinese Medicine 2008;27:209-12.
18. Zhao J, Wang L, Cao AL, et al. HuangQi Decoction Ameliorates Renal Fibrosis via TGF-β/Smad Signaling Pathway In Vivo and In Vitro. Cell Physiol Biochem 2016;38:1761-74.
19. Chang J, Ma C, Guo H, et al. Ultrafiltration Extract of Radix Angelica Sinensis and Radix Hedysari Attenuates Risk of Low-Dose X-Ray Radiation-Induced Myocardial Fibrosis In Vitro. Evid Based Complement Alternat Med 2021;2021:5580828.
20. Yao R, Cao Y, He YR, et al. Adiponectin attenuates lung fibroblasts activation and pulmonary fibrosis induced by paraquat. PLoS One 2015;10:e0125169.
21. Bloem AEM, Mostard RLM, Stoot N, et al. Perceptions of fatigue in patients with idiopathic pulmonary fibrosis or sarcoidosis. J Thorac Dis 2021;13:4872-84.
22. Nogawa H, Matsumoto Y, Tanaka M, et al. Diagnostic usefulness of bronchoscopy for peripheral pulmonary lesions in patients with idiopathic pulmonary fibrosis. J Thorac Dis 2021;13:6304-13.
23. Gao L, Tang H, He H, et al. Glycyrrhizic acid alleviates bleomycin-induced pulmonary fibrosis in rats. Front Pharmacol 2015;6:215.
24. Zhang Y, Zhang W, Zhang R, et al. Knockdown of FBLN2 suppresses TGF-β1-induced MRC-5 cell migration and fibrosis by downregulating VTN. Tissue Cell 2023;81:102005.
25. Otoupalova E, Smith S, Cheng G, et al. Oxidative Stress in Pulmonary Fibrosis. Compr Physiol 2020;10:509-47.
26. Veith C, Boots AW, Idris M, et al. Redox Imbalance in Idiopathic Pulmonary Fibrosis: A Role for Oxidant Cross-Talk Between NADPH Oxidase Enzymes and Mitochondria. Antioxid Redox Signal 2019;31:1092-115.
27. Estornut C, Milara J, Bayarri MA, et al. Targeting Oxidative Stress as a Therapeutic Approach for Idiopathic Pulmonary Fibrosis. Front Pharmacol 2021;12:794997.
28. Assayag M, Goldstein S, Samuni A, et al. 3-Carbamoyl-proxyl nitroxide radicals attenuate bleomycin-induced pulmonary fibrosis in mice. Free Radic Biol Med 2021;171:135-42.
29. Gungor H, Ekici M, Onder Karayigit M, et al. Zingerone ameliorates oxidative stress and inflammation in bleomycin-induced pulmonary fibrosis: modulation of the expression of TGF-β1 and iNOS. Naunyn Schmiedebergs Arch Pharmacol 2020;393:1659-70.
30. Shahzad M, Shabbir A, Wojcikowski K, et al. The Antioxidant Effects of Radix Astragali (Astragalus membranaceus and Related Species) in Protecting Tissues from Injury and Disease. Curr Drug Targets 2016;17:1331-40.
31. Zheng S, Ren W, Huang L. Geoherbalism evaluation of Radix Angelica sinensis based on electronic nose. J Pharm Biomed Anal 2015;105:101-6.
32. Zinellu A, Paliogiannis P, Sotgiu E, et al. Blood Cell Count Derived Inflammation Indexes in Patients with Idiopathic Pulmonary Fibrosis. Lung 2020;198:821-7.
33. Marzec JM, Nadadur SS. Inflammation resolution in environmental pulmonary health and morbidity. Toxicol Appl Pharmacol 2022;449:116070.
34. Sultan MT, Butt MS, Qayyum MM, et al. Immunity: plants as effective mediators. Crit Rev Food Sci Nutr 2014;54:1298-308.
35. Song S, Wang J, Liu G, et al. Protective Effects of the

 

Wenfei Buqi Tongluo Formula on the Inflammation in Idiopathic Pulmonary Fibrosis through Inhibiting the TLR4/MyD88/NF-κB Pathway. Biomed Res Int 2022;2022:8752325.
36. Yang S, Cui W, Wang M, et al. Bufei Decoction Alleviated Bleomycin-Induced Idiopathic Pulmonary Fibrosis in Mice by Anti-Inflammation. Evid Based Complement Alternat Med 2020;2020:7483278.
37. Kim MS, Baek AR, Lee JH, et al. IL-37 Attenuates Lung Fibrosis by Inducing Autophagy and Regulating TGF-β1 Production in Mice. J Immunol 2019;203:2265-75.
38. Liu Y, Zhong W, Zhang J, et al. Tetrandrine Modulates Rheb-mTOR Signaling-Mediated Selective Autophagy and Protects Pulmonary Fibrosis. Front Pharmacol 2021;12:739220.
39. Baek AR, Hong J, Song KS, et al. Spermidine attenuates bleomycin-induced lung fibrosis by inducing autophagy and inhibiting endoplasmic reticulum stress (ERS)-induced cell death in mice. Exp Mol Med 2020;52:2034-45.
40. Li N, Shi F, Wang X, et al. Silica dust exposure induces pulmonary fibrosis through autophagy signaling. Environ Toxicol 2021;36:1269-77.
41. Li X, Zhou J, Dou Y, et al. The protective effects of angelica organic acid against ox-LDL-induced autophagy dysfunction of HUVECs. BMC Complement Med Ther 2020;20:164.
42. Ma C, Wu H, Yang G, et al. Calycosin ameliorates atherosclerosis by enhancing autophagy via regulating the interaction between KLF2 and MLKL in apolipoprotein E gene-deleted mice. Br J Pharmacol 2022;179:252-69.
43. Yu JZ, Ying Y, Liu Y, et al. Antifibrotic action of Yifei Sanjie formula enhanced autophagy via PI3K-AKT-mTOR signaling pathway in mouse model of pulmonary fibrosis. Biomed Pharmacother 2019;118:109293.
44. Pei X, Zheng F, Li Y, et al. Niclosamide Ethanolamine Salt Alleviates Idiopathic Pulmonary Fibrosis by Modulating the PI3K-mTORC1 Pathway. Cells 2022;11:346.
45. Laha D, Deb M, Das H. KLF2 (kruppel-like factor 2 [lung]) regulates osteoclastogenesis by modulating autophagy. Autophagy 2019;15:2063-75.

**Cite this article as:** Sun C, Liu H, Chi B, Han J, Koga Y, Afshar K, Liu X. Improvement of idiopathic pulmonary fibrosis through a combination of *Astragalus* radix and *Angelica sinensis* radix via mammalian target of rapamycin signaling pathway-induced autophagy in rat. J Thorac Dis 2024;16(2):1397-1411. doi: 10.21037/jtd-24-28

 